fermentation

MDPI

Article

Seasonal Temperature Effects on EPS Composition and Sludge Settling Performance in Full-Scale Wastewater Treatment Plant: Mechanisms and Mitigation Strategies

Fei Xie [1], Chenzhe Tian [1], Xiao Ma [1], Li Ji [1], Bowei Zhao [2,*], Muhammad Ehsan Danish [1], Feng Gao [3] and Zhihong Yang [3]

[1] School of Environment and Resources, Taiyuan University of Science and Technology, Taiyuan 030024, China; xiefei@tyust.edu.cn (F.X.); 18335448609@163.com (C.T.); maxellmx@yeah.net (X.M.); jili@tyust.edu.cn (L.J.); ehsandanish310@gmail.com (M.E.D.)
[2] College of Civil Engineering, Taiyuan University of Technology, Taiyuan 030024, China
[3] Shanxi Zhengyang Sewage Purification Co., Ltd., Jinzhong 030600, China; xf03001@163.com (F.G.); 13934113751@126.com (Z.Y.)
* Correspondence: zhaobowei@tyut.edu.cn

Abstract

Seasonal temperature variations significantly impact biological wastewater treatment performance, particularly affecting extracellular polymeric substance (EPS) composition and sludge settling characteristics in activated sludge systems. This study investigated the temperature-induced EPS response mechanisms and their effects on nitrogen removal efficiency in a full-scale modified Bardenpho wastewater treatment plant, combined with laboratory-scale evaluation of EPS-optimizing microbial agents for performance enhancement. Nine-month seasonal monitoring revealed that when the wastewater temperature dropped below 15 °C, the total nitrogen (TN) removal efficiency decreased from 86.5% to 80.6%, with a trend of significantly increasing polysaccharides (PS) in dissolved organic matter (DOM) and loosely-bound EPS (LB-EPS) and markedly decreasing tightly-bound EPS (TB-EPS). During the low-temperature periods, when the sludge volume index (SVI) exceeded 150 mL/g, deteriorated settling performance could primarily be attributed to the reduced TB-EPS content and increased LB-EPS accumulation. Microbial community analysis showed that EPS secretion-promoting genera of *Trichococcus*, *Terrimonas*, and *Defluviimonas* increased during the temperature recovery phase rather than initial temperature decline phase. Laboratory-scale experiments demonstrated that EPS-optimizing microbial agents dominated by *Mesorhizobium* (54.2%) effectively reduced protein (PN) and PS contents in LB-EPS by 70.2% and 54.5%, respectively, while maintaining stable nutrient removal efficiency. These findings provide mechanistic insights into temperature–EPS interactions and offer practical technology for improving winter operation of biological wastewater treatment systems.

Keywords: activated sludge; extracellular polymeric substances; temperature effects; nitrogen removal; sludge settling

Academic Editor: Massimiliano Fabbricino

Received: 27 July 2025
Revised: 5 September 2025
Accepted: 7 September 2025
Published: 12 September 2025

Citation: Xie, F.; Tian, C.; Ma, X.; Ji, L.; Zhao, B.; Danish, M.E.; Gao, F.; Yang, Z. Seasonal Temperature Effects on EPS Composition and Sludge Settling Performance in Full-Scale Wastewater Treatment Plant: Mechanisms and Mitigation Strategies. *Fermentation* **2025**, *11*, 532. https://doi.org/10.3390/fermentation11090532

1. Introduction

Biological wastewater treatment has become the predominant approach for municipal wastewater management worldwide, with activated sludge processes accounting for approximately 80% of wastewater treatment plants (WWTPs) globally [1]. These systems rely

on complex microbial communities to degrade organic pollutants and remove nutrients through biochemical processes [2,3]. Among various biological treatment technologies, the activated sludge process, including variations such as the A/B process, sequencing batch reactor (SBR), and oxidation ditch systems, has gained widespread adoption due to its technological maturity and proven effectiveness. The fundamental principle involves creating optimal conditions for microorganisms to metabolize organic matter, convert complex pollutants into simpler compounds, and achieve water quality standards.

The operational performance of activated sludge systems is significantly influenced by environmental factors, particularly by temperature [4]. In northern regions characterized by continental climates, seasonal temperature variations pose substantial challenges to WWTP operations [5]. Low-temperature impacts on WWTPs manifest as various operational problems. Research has shown that over 50% of WWTPs experience sludge bulking phenomena during winter [6]. Winter temperatures (below −15 °C) create adverse conditions that significantly impact microbial physiology and biochemical processes. The relationship between settling performance, temperature effects, and functional microbial response mechanisms at temperatures below 15 °C remains poorly understood, particularly in full-scale operational environments [7]. These temperature fluctuations affect multiple operational parameters, including dissolved oxygen, nutrient availability, pH stability, and microbial metabolic activity. Lower temperatures generally inhibit microbial activity and result in decreased contaminant removal efficiency [8]. These challenges are compounded by the need to maintain consistent effluent quality standards regardless of seasonal variations.

Extracellular polymeric substances (EPS) play a crucial role in activated sludge processes, representing 60–80% of total sludge composition and serving as the primary factor maintaining sludge stability and physical properties [9]. EPS consist of proteins (PN), polysaccharides (PS), nucleic acids, and lipids secreted by microorganisms, forming a complex matrix that binds cells together in floc structures. These substances are essential for nitrogen removal processes, influencing critical operations including sludge settling, dewatering, and drying [10]. Sludge settling and dewaterability parameters are intrinsically linked to EPS composition and distribution. The sludge volume index (SVI), capillary suction time, and specific resistance to filtration are directly influenced by the protein-to-polysaccharide ratio in different EPS fractions [11,12]. Tightly-bound EPS (TB-EPS) contribute to floc stability and enhanced settling, while excessive loosely-bound EPS (LB-EPS) can deteriorate solid–liquid separation through increased sludge hydrophilicity and reduced floc density [13].

Beyond their structural role, EPS undergo complex fate and transformation processes that significantly impact treatment performance. Soluble microbial products (SMP), consisting of biomass-associated products released during substrate metabolism and biomass decay, interact closely with EPS components and contribute to effluent quality variations [14,15]. The fate of EPS involves multiple pathways including enzymatic hydrolysis by extracellular enzymes, biological uptake and utilization by heterotrophic bacteria, and physical entrapment within sludge flocs [16]. These transformation processes are particularly sensitive to temperature variations, with hydrolysis rates decreasing exponentially at temperatures below 15 °C [17]. Under nutrient-limited conditions, EPS serves as an energy storage mechanism, providing carbon and energy sources for microbial metabolism during periods of substrate scarcity [18]. Temperature variations significantly affect both EPS production and composition [19]. During low-temperature periods, microorganisms alter their EPS secretion patterns as an adaptive response to environmental stress. This temperature-induced EPS modification directly impacts sludge settling characteristics and overall system performance. When sludge return ratios are increased to maintain adequate biomass concentrations in biological reactors, the resulting decrease in food-to-

microorganism ratios (F/M) can trigger excessive filamentous bacterial growth, leading to sludge bulking and poor solid–liquid separation in secondary clarifiers [20]. Additionally, increased sludge reflux ratios reduce waste sludge production, extend sludge age and further promote filamentous growth and sludge aging phenomena. Full-scale WWTPs present complex operational challenges with dynamic microbial community structures that respond to multiple environmental variables simultaneously [21]. Limited research exists on EPS temperature response mechanisms and their effects on sludge performance in actual treatment facilities, hindering comprehensive understanding of seasonal performance variations. This knowledge gap impedes the development of effective operational strategies for maintaining consistent treatment performance throughout the year. Some studies have investigated the effects of temperature and climate change on the nitrogen removal performance of WWTPs [22], but there is a lack of in-depth understanding of the EPS response mechanism. Current research on the response mechanism of EPS to temperature in full-scale treatment facilities and its effect on sludge performance is limited. Particularly, the inner connection of microbial communities, EPS, and nitrogen removal under seasonal temperature variations remains unclear. This hinders a comprehensive understanding of seasonal performance fluctuations and impedes the development of effective operational strategies to maintain stable year-round operation of WWTPs.

This research addresses critical knowledge gaps in understanding EPS-mediated temperature effects on full-scale wastewater treatment performance. The study objectives include comprehensive monitoring of seasonal variations in pollutant removal efficiency, detailed characterization of EPS composition and production patterns, analysis of microbial community structure changes, and evaluation of potential enhancement strategies using specialized microbial agents. Through combined field monitoring and laboratory-scale reactor studies, this work aims to elucidate the fundamental mechanisms governing seasonal performance variations and develop practical solutions for improving winter operation of biological wastewater treatment systems.

2. Methodology

2.1. Full-Scale and Lab-Scale Wastewater Treatment Process

2.1.1. Full-Scale Wastewater Treatment Process

The study conducted experiments at a full-scale WWTP based on the modified Bardenpho process (Figure 1a). This process builds on the Anaerobic-Anoxic-Oxic (A^2/O) process by adding a post-anoxic tank and a post-oxic tank at the end of the oxic tank to enhance the diversity of the treatment process. This modification allows functional microorganisms to further utilize nutrients in the effluent from the conventional oxic tank, achieving the goal of optimizing the traditional process and improving treatment efficiency.

During the monitoring period, the daily wastewater treatment capacity of the plant ranged from 47,275 m^3/d to 110,899 m^3/d (Table 1). Of the influent to the biochemical tanks, 30% entered the pre-anoxic tank, while the remaining 70% entered the anoxic tank. The sludge retention time (SRT) of the WWTP was controlled at approximately 16 days. The reflux ratio of nitrification (internal reflux ratio) ranged from 250% to 300%, and the return activated sludge (RAS) ratio (external reflux ratio) ranged from 80% to 100%. The external reflux ratio could be directed to both the pre-anoxic tank and the anaerobic tank. An external carbon source, sodium acetate, was supplemented at the front of the anoxic tank. The dosage of sodium acetate was adjusted according to the influent TN concentration, with a typical dosage of 50–80 mg/L (as COD) to maintain the anoxic zone C/N ratio above 8.

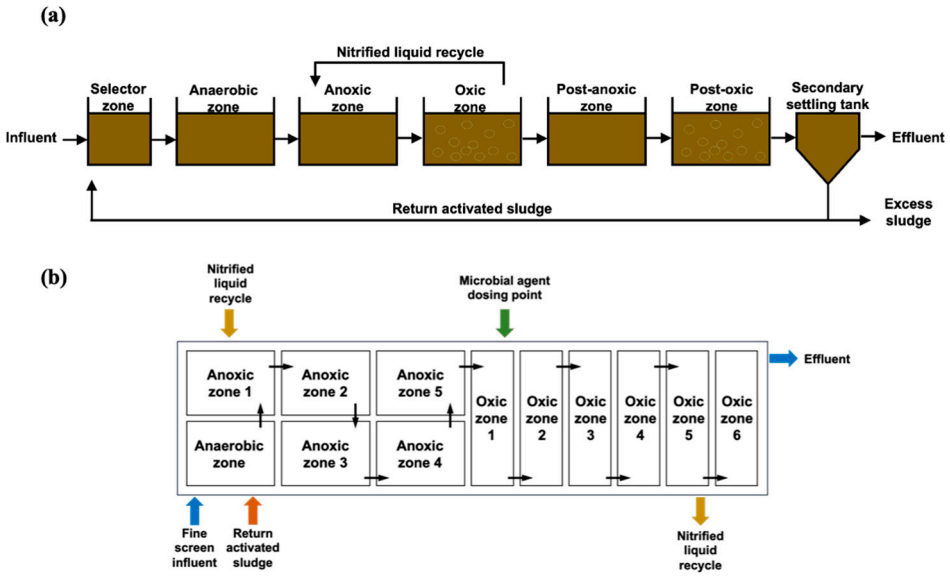

Figure 1. Process flow diagram of the WWTP (**a**) and A^2O reactor in laboratory scale (**b**).

Table 1. Operational parameters comparison between full-scale WWTP and laboratory reactor.

Parameter	Full-Scale WWTP	Laboratory Reactor
Total volume	~15,000 m^3	180.3 L
Treatment capacity	47,275–110,899 m^3/d	7.2 L/d
Anaerobic HRT (h)	4.5	2.0
Anoxic HRT (h)	8.0	10.6
Oxic HRT (h)	12.0	12.9
SRT (h)	~16	~15
Internal reflux ratio (%)	250–300	300
External reflux ratio (%)	80–100	100
Temperature (°C)	12–25	18–22

2.1.2. Lab-Scale Wastewater Treatment Process

A lab-scale experiment was conducted to test the optimization of EPS microbial agents. The experiment utilized a customized A^2/O reactor with a total volume of 180.3 L, consisting of an anaerobic zone with one corridor (volume of 14.9 L), an anoxic zone with five corridors (each with a volume of 14.9 L, totaling 74.3 L), and an oxic zone with six corridors (each with a volume of 15.2 L, totaling 91.1 L). The influent was sourced from the inlet wastewater of the fine screen at a certain WWTP. Activated sludge was inoculated from the reflux sludge of the WWTP, with the external reflux ratio controlled at a ratio of 100%. Nitrification reflux was managed using three peristaltic pumps, with the internal reflux ratio adjusted to a ratio of 300%. The discharge rate of excess sludge was approximately 5%. The hydraulic retention times (HRT) of the reactor were approximately 2 h for the anaerobic zone, 10.6 h for the anoxic zone, and 12.9 h for the oxic zone. A schematic diagram of the reactor is provided in Figure 1b. The laboratory reactor was operated at controlled conditions: temperature 20 ± 2 °C using external heating, and pH maintained at 7.0–7.6 through automatic control. Specifically, a pH controller connected to two peristaltic pumps was employed. When the pH dropped below 7.0, 0.1 mol/L sodium hydroxide (NaOH) solution was dosed to raise the pH; when the pH exceeded 7.6, 0.1 mol/L hydrochloric acid (HCl) solution was added to lower the pH. Dissolved oxygen in the oxic zone was maintained at 3–5 mg/L using fine bubble aeration, anoxic zones were maintained at <0.5 mg/L, and the anaerobic zone at <0.2 mg/L.

The experimental operation was divided into three stages: the commissioning stage (days 1 to 9 of reactor operation), the stable operation stage (days 10 to 15 of reactor operation), and the microbial agent dosing stage (days 16 to 21 of reactor operation). During each stage, the concentrations of relevant pollutants, activated sludge characteristics, and changes in the microbial community structure of the sludge in each zone of the reactor were monitored and analyzed. The microbial agents used in this study were cultivated through autonomous domestication, with a dosage of 2000 g/m^3.

2.2. Chemical Analysis

The experimental period lasted approximately 9 months, with a sampling frequency of once per week. The experimental tests included pollutants such as chemical oxygen demand (COD), ammonia nitrogen (NH_4^+-N), total nitrogen (TN), total phosphorus (TP), and five-day biochemical oxygen demand (BOD_5) in the total influent and effluent of the WWTP [23]. Water quality parameters were analyzed according to standard methods for the examination of water and wastewater [24]. The total influent sampling point was located at the treatment unit after primary treatment, while the total effluent was collected from the end of the secondary sedimentation tank. The units between influent and effluent included all biological treatment stages. The experiment simultaneously tested the reflux activated sludge samples from the WWTP, with sampling times consistent with pollutant testing. The main parameters measured were mixed liquor suspended solids (MLSS), mixed liquor volatile suspended solids (MLVSS), and SVI. MLSS and MLVSS were determined gravimetrically following standard methods [24]. SVI was measured by settling 1 L of mixed liquor in an Imhoff cone for 30 min at 20 °C ± 2 °C, calculated as SVI (mL/g) = (settled sludge volume in mL × 1000)/MLSS (mg/L). Samples with typical temperature differences, specifically the reflux activated sludge from before, during, and after the winter cold wave period, were selected for microbial community testing. The functional relationship analysis of related parameters was conducted using SPSS R26 and Origin 2024.

The heat extraction method was used to extract different forms of EPS [18], including dissolved organic matter (DOM), LB-EPS, and TB-EPS. Briefly, sludge samples were centrifuged at 4000 rpm for 15 min, and the supernatant was collected as DOM. The pellet was resuspended in 0.05% NaCl solution and heated at 70 °C for 30 min, then centrifuged at 4000 rpm for 15 min to obtain LB-EPS. The remaining pellet was resuspended in 0.05% NaCl and heated at 60 °C for 30 min, followed by centrifugation at 12,000 rpm for 20 min to extract TB-EPS.

The fluorescence characteristics of the EPS samples were determined using a fluorescence spectrophotometer. The experiment set the excitation wavelength (Ex) range from 200 to 450 nm, with data collection intervals of 5 nm; the emission wavelength (Em) range was from 200 to 600 nm, with a data collection interval of 2 nm. Simultaneously, the slit width was set to 5 nm, and the scanning speed was 6000 nm/min. To eliminate Raman scattering interference, distilled water was used as a blank reference, and Matlab R2020b was employed to correct Raman and Rayleigh scattering. The relative fluorescence intensity (RFU) was used as the normalization unit for fluorescence data. The PN and PS values in EPS were determined according to Bian, et al. [25].

2.3. Metagenomic Sequencing

High-throughput 16S rRNA gene amplicon sequencing was performed using primers 338F (5′-ACTCCTACGGGAGGCAGCAG-3′) and 806R (5′-GGACTACHVGGGTWTCTAAT-3′) targeting the V3-V4 hypervariable regions. Operational taxonomic units (OTUs) were clustered at 97% sequence similarity using the UPARSE algorithm in QIIME 2. Although

amplicon sequence variants (ASVs) represent the current best practice, OTU clustering at 97% similarity was selected to enable comparison with the existing literature data from similar wastewater treatment systems and to maintain consistency with our laboratory's historical datasets. The specific sampling dates are shown in Table S1.

3. Results and Discussion

3.1. Removal Efficiency of Nutrients

3.1.1. Seasonal Nutrients Removal Performance

The effluent indicators of the wastewater treatment plant were relatively stable, with annual average effluent concentrations of COD, NH_4^+-N, TN, and TP being 24.57 ± 3.21 mg/L, 0.28 ± 0.05 mg/L, 8.85 ± 1.12 mg/L, and 0.31 ± 0.04 mg/L, respectively. Table 2 shows the maximum and minimum values of various effluent indicators throughout the year. Due to the WWTP location in a mid-to-high latitude region, annual wastewater temperature variations were significant. Starting from day 50 of this experimental testing, a continuous declining trend was observed, with water temperature gradually decreasing from 20 °C to 12.5 °C. Water temperature began to rise again from day 154 of testing. By day 225 of testing, the wastewater temperature had recovered to 20 °C, indicating that the WWTP experienced 104 days of relatively low-temperature conditions, and exhibiting a distinct pattern of initial cooling followed by warming. The period from day 125 to day 155 represented the coldest winter period, with an average temperature of 12.6 °C.

Table 2. Maximum and minimum values of effluent indicators.

Indicators	pH	SS	COD	BOD_5	NH_4^+-N	TN	TP
Max (mg/L) [1]	7.6	8.0	46.0	6.1	4.39	14.24	0.59
Min (mg/L) [1]	6.3	2.0	12.0	1.1	0.02	2.30	0.02
Effluent limit [2] (mg/L)	6–9	10	50	10	5	15	0.5
Compliance rate [3] (%)	100	100	100	100	100	98	99

[1] Values represent daily measurements over the 9-month monitoring period; [2] Based on the "Discharge Standard of Pollutants for Municipal Wastewater Treatment Plants" (GB 18918-2002, China, Grade A) [26]; [3] Percentage of daily samples meeting the Grade A effluent limit during the 9-month monitoring period.

3.1.2. Seasonal Effects of Nutrients Removal Performance

The impact of wastewater temperature variations on nutrient removal efficiency in the biochemical tank is illustrated in Figure 2. Throughout the 9-month monitoring period, the highest monthly average temperature in the biochemical tank occurred in August at 25.4 ± 1.2 °C, while the lowest monthly average temperature was recorded in January at 12.4 ± 0.8 °C. During January, when the monthly average wastewater temperature was at its minimum, the monthly average TN removal efficiency was 83.2 ± 2.1%. Subsequently, as wastewater temperature gradually increased, TN removal efficiency also improved progressively, reaching the highest annual monthly average TN removal efficiency of 86.5 ± 1.8% in March when the average wastewater temperature reached 14.6 °C. This finding is consistent with results reported in other studies [27]. As the biochemical tank wastewater temperature continued to rise thereafter, TN removal efficiency remained relatively stable, consistently maintaining levels above the January average level. Temperature elevation may influence dissolved oxygen and microbial community dynamics in aerobic biological treatment processes [22]. When wastewater temperature first declined in September, TN removal efficiency experienced a significant drop to 80.6 ± 2.7%, representing the lowest annual monthly average efficiency. This indicates that nitrifying and denitrifying bacteria are highly sensitive to temperature fluctuations, exhibiting stress-like responses [28]. Furthermore, under low-temperature conditions, the growth rate of nitrite-oxidizing bac-

teria (NOB) exceeds that of ammonia-oxidizing bacteria (AOB), potentially resulting in NO_3^--N accumulation and compromised nitrogen removal performance [29]. Although wastewater temperature continued to decrease subsequently, TN removal efficiency did not decline further and gradually recovered. This suggests that most nitrifying and denitrifying bacteria exhibit strong adaptability and can adequately adjust to low-temperature environments [30].

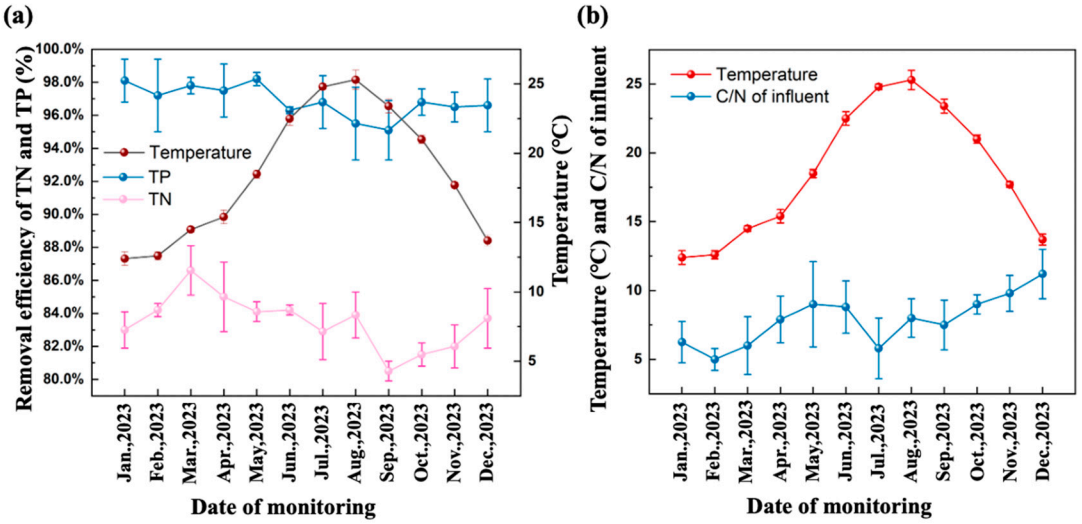

Figure 2. Annual variation of nutrients removal efficiency (**a**), wastewater temperature, and influent C/N ratio (**b**).

The biochemical tank consistently demonstrated excellent TP removal performance, maintaining removal efficiencies above 95% throughout the year. Treatment effectiveness remained at satisfactory levels even during periods of lower wastewater temperatures. However, decreased TP removal efficiency was observed during the higher temperature months of August and September. Therefore, it is hypothesized that TP removal efficiency is not significantly influenced by wastewater temperature.

The impact of C/N ratio variations on nutrient removal efficiency is presented in Figure 2b. During the annual monitoring period, the highest monthly average influent C/N ratio occurred in December at 11.6, while the lowest was recorded in February at 5.0. Throughout most of the year, the influent C/N ratio remained within the 6.0–9.0 range, which represents the optimal C/N ratio range for wastewater treatment. During January through March, the influent C/N ratio remained stable while the TN removal efficiency increased. From March to May, the C/N ratio continuously increased while the TN removal efficiency exhibited a declining trend, confirming that changes in influent C/N ratio were not the primary factor influencing TN removal efficiency variations. This is attributed to the fact that the influent C/N ratio consistently remained within a relatively suitable range that does not impede the denitrification process. TP removal efficiency maintained relatively stable levels during the January–May monitoring period, while the influent C/N ratio significantly increased during this timeframe. From May to September, TP removal efficiency exhibited considerable fluctuations with overall deteriorated performance, followed by rapid recovery and stabilization from September to December, concurrent with a gradual increase in influent C/N ratio. Overall, changes in influent C/N ratio did not significantly influence TP removal efficiency. Under seasonal temperature variations, the system consistently maintained effective COD removal, benefiting from robust bacterial adhesion and energy storage capabilities within the system [30].

3.2. Components and Characteristics of EPS

3.2.1. Changes in EPS Components During Temperature Fluctuations

Under low-temperature conditions of 15 °C, the PS in DOM and LB-EPS of activated sludge both exhibited an upward trend with decreasing temperature, while TB-EPS demonstrated the opposite trend (Figure 3). Compared to PN, the overall PS was relatively low, whereas most conventional A^2/O processes exhibit higher PS in EPS [31]. This phenomenon is primarily attributed to the high COD utilization efficiency of the WWTP, particularly due to the modified process incorporating additional post-anoxic and post-oxic tanks, which enables recovery of recalcitrant organic matter and carbon sources from deceased microorganisms in the effluent activated sludge from the oxic section. Through endogenous denitrification processes, nutrients required for microbial growth and metabolism are fully utilized, while the efficiency and rate of microbial conversion of dissolved organic carbon to extracellular PN are lower than those for PS conversion [18]. During the monitoring period, both PS in DOM and LB-EPS showed significant increases on day 141, reaching 2.4 ± 0.3 mg/gVSS and 6.7 ± 0.5 mg/gVSS, respectively, when the wastewater temperature was 12.5 °C. However, PS in TB-EPS changes were not pronounced. In the anoxic tank, PS exhibited notable increases in DOM and LB-EPS during early February when temperatures were lowest, while TB-EPS showed a significant decline, reaching a minimum value of 18.01 ± 1.42 mg/gVSS before rapidly recovering to normal levels. The PS in DOM and LB-EPS of the oxic tank increased similarly to the anoxic zone under low-temperature conditions, while TB-EPS remained relatively unaffected by low temperatures and maintained stable levels.

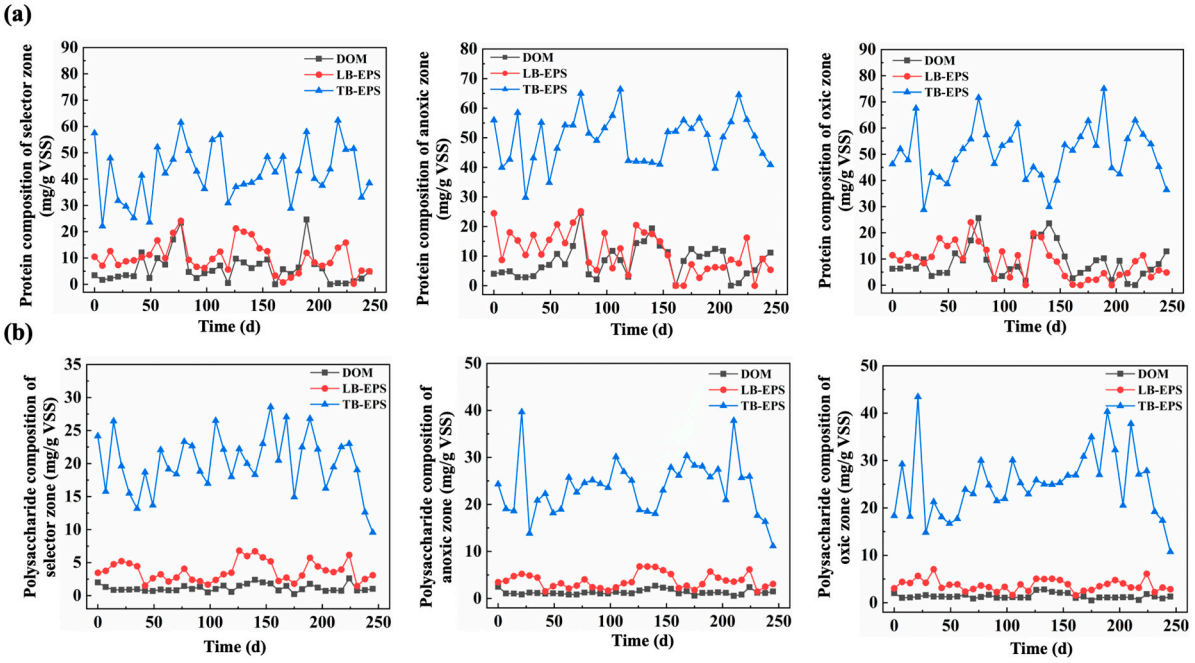

Figure 3. PN composition (**a**) and PS (**b**) composition in the selection, anoxic, and oxic tanks.

TB-EPS consistently exhibited the highest PN content among all components (Figure 3). When wastewater temperature dropped below 15 °C, PN in TB-EPS of the selector, anoxic tank, and oxic tank decreased significantly with declining temperature, while PN in DOM and LB-EPS showed increasing trends. For example, in the selector tank, PN in TB-EPS decreased from 44.1 mg/gVSS to 30.9 mg/gVSS when temperature dropped below 15 °C. The addition of post-anoxic and post-oxic sections enhanced COD utilization efficiency, resulting in relatively low carbon, nitrogen, and phosphorus content in the selector, anoxic, and oxic zones. Consequently, the microbial EPS synthesis process was minimally affected

and demonstrated strong adaptability to adverse low-temperature environments, with relatively subtle change patterns. Therefore, the efficiency and rate of microbial conversion of dissolved organic carbon to extracellular PN remained lower than those for PS conversion. Research indicates that the optimal temperature for EPS production is approximately 25−31 °C, while conditions below 15 °C inhibit the EPS biosynthesis process [32]. When the temperatures dropped below 15 °C, PN accumulated substantially across all components, but a significant increase of PN in LB-EPS was only detected during the lowest temperatures. The variation trends of PN in the anoxic tank indicate that when the temperature first dropped below 15 °C, PN accumulated substantially across all EPS components. During the lowest water temperatures, PN in DOM and LB-EPS accumulated extensively, while TB-EPS showed marked decreases.

3.2.2. Effect of PS on Nutrients Removal Efficiency

To minimize the influence of temperature variations, the changes in PS content and nutrients concentrations during the monitoring period from day 125 to day 155 were analyzed (Figure 4). During various stages, PS in DOM and LB-EPS increased significantly, while PS in TB-EPS decreased markedly. Related influent parameters showed minimal variation, but corresponding effluent indicators exhibited notable fluctuations. The effluent of NH_4^+-N and COD demonstrated considerable changes, while TN effluent showed no significant fluctuations, indicating that changes in PS had certain effects on effluent NH_4^+-N and COD. The increase in PS in DOM and LB-EPS and the significant decrease in PS in TB-EPS may have influenced the nitrification process, but showed no apparent impact on the denitrification process in the anoxic tank. The abnormal increase in effluent COD may result from deteriorated sludge adsorption capacity for COD due to changes in PS across various EPS components, leading to elevated effluent COD concentrations. PS, serving as microbial reserve resources, can enhance adhesion performance and influence COD removal efficiency [25]. Furthermore, changes in PS across various sludge EPS components showed no significant impact on TP removal efficiency.

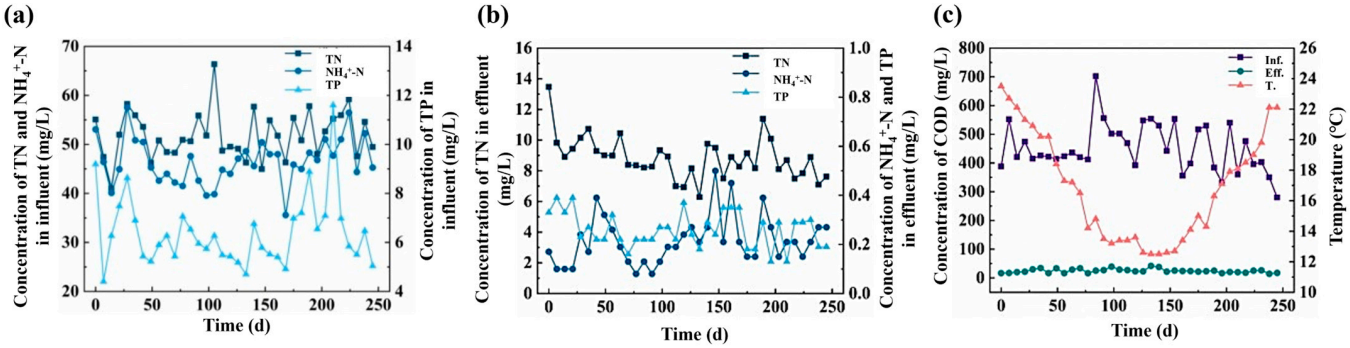

Figure 4. Nutrients concentration in influent (**a**) and effluent (**b**), and COD concentration and wastewater temperature (T.) of the WWTP (**c**).

3.2.3. EPS and Sludge Settleability

The characteristics of activated sludge were assessed through monitoring indicators including MLSS and MLVSS (Figure 5). The SVI exhibited notable variations with temperature changes. When wastewater temperature dropped below 20 °C (days 50–154), SVI values consistently exceeded 150.0 mL/g, averaging 159.2 ± 12.4 mL/g, indicating that deteriorated sludge settleability was primarily attributed to significant temperature reduction. Although the total quantity of excess sludge was relatively low, effluent quality consistently met discharge standards. This performance is mainly related to the modified

process configuration incorporating pre-anoxic tanks, post-anoxic tanks, and post-oxic tanks, which enhanced removal efficiency of nutrients through extended process flow.

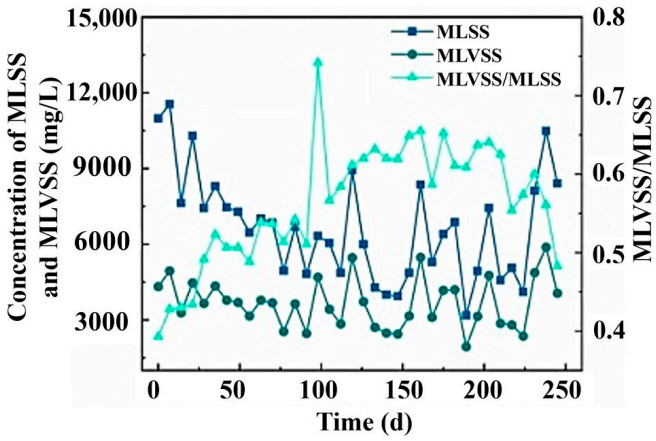

Figure 5. The MLSS, MLVSS, and MLSS/MLVSS of the return sludge.

To analyze the impact of EPS variations on nutrient removal performance, two periods with relatively stable temperatures were selected: days 85–120 and days 125–155, with average wastewater temperatures of 13.7 °C and 12.6 °C, respectively. The choice relied on three factors, not just temperature stability. These periods represent "mild" and "severe" low-temperature stages (critical < 15 °C threshold for microbial activity/EPS secretion). The stable temperatures within each period avoid erratic shift interference. Additionally, they exhibit synchronous trends between temperature, nutrient removal, and sludge settleability. This synchrony focuses analysis on EPS as the key mediator between temperature and system performance. The operational parameters remained stable across both periods, with no abnormal adjustments. This eliminates operational confounders, ensuring that EPS and performance changes trace to temperature.

During the initial stage when wastewater temperature dropped just below 15 °C (days 85–120), SVI showed minimal fluctuation, indicating that biochemical tank sludge settling performance remained relatively stable. MLSS and MLVSS values began to increase gradually. Within optimal temperature ranges, microorganisms can more effectively decompose organic matter. However, microbial growth and metabolism is inhibited under low-temperature conditions, which led to the organic matter becoming adsorbed by activated sludge, not being metabolized promptly by microorganisms. As a result, an increased organic matter content and elevated excess sludge quantities were observed. During this period, PS and PN in all components of EPS increased, enhancing organic matter content in the activated sludge and causing the MLSS/MLVSS ratio to increase significantly from 51.4 ± 3.2% to 61.2 ± 4.1%.

During the coldest winter phase (days 125–155), MLSS and MLVSS values gradually decreased, indicating that excess sludge quantities were synchronously reduced due to declining temperatures. Influent organic matter content showed no significant changes. It is hypothesized that microbial activity was substantially weakened during this period, resulting in markedly reduced excess sludge production. The satisfactory effluent quality was attributed to the lower sludge loading, which effectively adsorbed and degraded most organic matter. Notably, the MLSS/MLVSS ratio exhibited minimal fluctuations during this period. Component analysis revealed significant increases in PS and PN in DOM and LB-EPS, while PS and PN in TB-EPS decreased markedly. LB-EPS and TB-EPS possess strong binding and flocculation capabilities, which contribute to the retention of dominant bacterial genera [25]. Under these extreme low-temperature conditions, SVI increased significantly, reaching a maximum of 198 mL/g. Research has demonstrated that

excessive LB-EPS can weaken floc structure and impair sludge-water separation [33]. It is hypothesized that the decrease in TB-EPS under low-temperature conditions, coupled with increased DOM and LB-EPS, further reduces sludge floc density, representing the primary cause of deteriorated sludge settling performance. Pearson correlation analysis revealed significant negative correlation between TB-EPS content and SVI ($r = -0.72$, $p < 0.01$), while LB-EPS showed a positive correlation with SVI ($r = 0.68$, $p < 0.01$). These results confirm that the decrease in TB-EPS and increase in LB-EPS are the key factors leading to deteriorated sludge settling performance. However, we acknowledge that direct floc structure measurements (microscopy, particle size analysis) would strengthen these correlations and represent an area for future investigation.

3.3. Structure of Microbial Community

3.3.1. Overall Analysis of Illumina Sequence Data

The rarefaction curves for the diversity index Sobs (observed richness) all approached a plateau, indicating that the sequencing data volume was reasonable. The Coverage index (community coverage) for all sequencing samples was 0.99, and an increase in this value indicates enhanced probability of sequence detection in samples while reducing the likelihood of undetected sequences. This demonstrates that the current sequencing covered most OTUs, with relatively complete representation of microbial information, providing relatively accurate reflection of sequencing and analytical results while offering strong support for the rationality of the sequencing work [34].

Most samples with wastewater temperatures below 15 °C exhibited Sobs values lower than 2000, indicating that temperature has a pronounced impact on the number of microbial community species in the biochemical tank. Conversely, when temperatures exceeded 15 °C, the biochemical tank maintained higher microbial biomass, which contributes to enhanced microbial degradation capacity for nutrients. The Shannon index serves as one of the important indicators for estimating microbial diversity in samples. Higher index values indicate greater community diversity. It was revealed that sludge community diversity was relatively lower during the cold water temperature period from November 2023 to March 2024 compared to other timeframes. Both the Chao index and ACE index are commonly used indices for evaluating OTU numbers in samples. When wastewater temperature first dropped below 15 °C but remained above 13 °C, the total species count in the biochemical tank initially showed a significant decline followed by subsequent recovery. However, after temperature dropped below 13 °C, the total species count in the biochemical tank decreased again, followed by gradual recovery to relatively stable levels. This demonstrates that significant temperature reduction or the initial decline to a critical threshold below 15 °C directly results in decreased total species count in the biochemical tank, but after a period of time, the species count recovers to relatively stable levels. This indicates that the microbial community in the biochemical tank possesses excellent low-temperature adaptability and can rapidly mitigate the adverse effects of low temperatures.

At the phylum level, the microbial community primarily comprised seven major phyla: Pseudomonadota, Bacteroidota, Chloroflexota, Bacillota, Actinomycetota, Patescibacteria, and Acidobacteriota, all of which exhibited notable variations throughout the sludge samples (Figure 6). Pseudomonadota, with Pseudomonas as its type genus, represents a renamed classification following the removal of Epsilonproteobacteria, Deltaproteobacteria, and Oligoflexia from the former Proteobacteria phylum, and occupies an absolutely dominant position in activated sludge within oxic tanks. This phylum contains numerous aerobic bacteria which can efficiently utilize organic matter to synthesize polyhydroxyalkanoates (PHA) and significantly reduce COD in wastewater [35]. Bacteroidota can enhance the degradation capacity of macromolecular organic compounds and serves as

the phylum for denitrifying bacteria, promoting nitrogen cycling. Chloroflexota consists predominantly of filamentous bacteria, with some species capable of performing anaerobic photosynthesis [36]. Actinomycetota is frequently associated with sludge bulking phenomena.

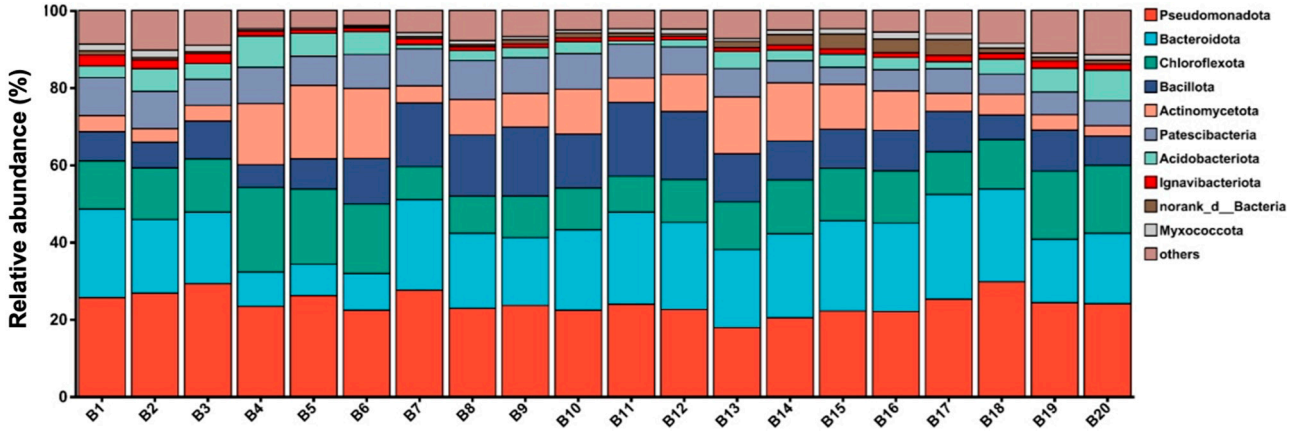

Figure 6. Changes in microbial structure at the phylum level.

3.3.2. Microbial Structure at the Genus Level Under Cold Waves

Wastewater temperature variations significantly affect activated sludge performance and nutrients removal efficiency. Samples B4 (day 63, pre-cold wave), B5 (day 77, during cold wave), and B6 (day 91, post-cold wave) were selected for functional classification of major bacterial genera to analyze the impact of low temperatures on major functional microbial communities at the genus level. The test results for major functional microbial communities at the genus level are presented in Figure 7a. The functional bacterial primarily include EPS secretion-promoting genera [37,38], polyphosphate-accumulating organisms (PAOs) [39,40], filamentous bacteria (FB) [41], denitrifying polyphosphate-accumulating organisms (DPAOs) [42], nitrifying bacteria (NB) [43], and denitrifying bacteria (DNB) [44,45]. EPS secretion-promoting genera are primarily associated with the capacity to promote microbial secretion and production of EPS-related components.

The abundance of *Trichococcus* did not directly increase with temperature decline, but significantly increased during the late cold wave period when temperatures began to recover, rising dramatically from 3.56% in B5 to 6.04% in sample B6. *Trichococcus* facilitates denitrification processes under cold conditions [30]. *Trichococcus* can degrade various carbohydrates and possesses a large number of cold shock domains (CSD), enabling it to maintain normal metabolic activities at low temperatures [46]. Furthermore, three other genera of *Terrimonas*, *Defluviimonas*, and *Ferruginibacter* all exhibited similar variation trends to *Trichococcus*, and their abundances increased from 2.45%, 1.04%, and 0.73% in B5 to 2.98%, 1.14%, and 0.89% in B6, respectively. The EPS secretion bacteria of *Terrimonas* increased in association with improved reactor performance, indicating its crucial role in resisting cold wave impacts [47]. This microbial community analysis conclusion is consistent with EPS composition findings, namely that increased EPS secretion by microorganisms in sludge occurs during temperature recovery following low-temperature exposure. This phenomenon is attributed to the modified process configuration with relatively abundant biological treatment units, which not only enhances nutrient removal efficiency but also mitigates the impact of low temperatures on activated sludge. Additionally, FB in sludge samples exhibited similar variation trends, with bacterial species not immediately increasing with temperature decline; however, their abundances increased from 2.24% in B5 to 4.02% in B6 when temperatures began to recover, further validating the EPS analysis conclusions.

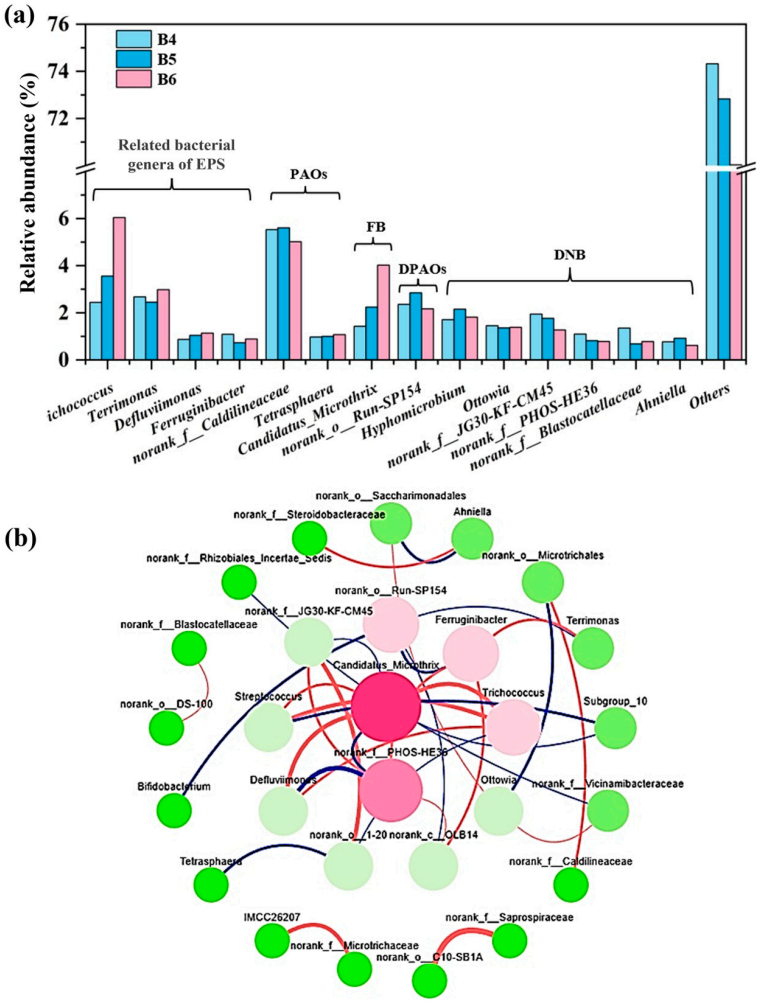

Figure 7. Major functional microbial communities at the genus level (**a**) and ecological correlation network diagram (**b**).

By calculating correlation coefficients among various bacterial genera and connecting significantly correlated genera nodes, a network analysis diagram was constructed (Figure 7b). The number of connections between different bacterial genera indicates the closeness of relationships between the current genus and other genera within the microbial community, while the thickness of connections represents the strength of correlations between different genera. Red connections represent positive correlations, while blue connections represent negative correlations. *Candidatus_Microthrix* (belonging to FB bacteria) and *norank_f__PHOS-HE36* (belonging to DNB bacteria) serve as hub genera, exhibiting the closest relationships with other bacterial genera. Notably, *Candidatus_Microthrix* demonstrated extremely strong positive correlations with EPS secretion-promoting genera *Trichococcus* and *Defluviimonas*, indicating distinct mutualistic symbiotic relationships between FB bacteria and EPS secretion-promoting genera. Conversely, *norank_f__PHOS-HE36* exhibited extremely strong negative correlations with FB bacterium *Candidatus_Microthrix* and EPS secretion-promoting genus *Defluviimonas*, suggesting significant competitive relationships between certain denitrifying bacteria and FB bacteria as well as EPS secretion-promoting genera. Therefore, it is hypothesized that appropriately enhancing the abundance of DNB bacterium *norank_f__PHOS-HE36* in sludge could mitigate the accumulation of sludge LB-EPS and DOM, reduce SVI, and improve the settling performance of activated sludge in biological treatment units during low-temperature periods to some extent.

3.4. Effect of the EPS-Optimizing Microbial Agents on Temperature Shock Resistance

3.4.1. Effect of the Microbial Agents on Nutrients Removal Efficiency

Excessive EPS under low-temperature conditions reduces sludge settling performance. To improve sludge settling performance in winter, a novel sludge reduction microbial agent was applied to reduce excess sludge concentration and lower sludge treatment costs. Illumina sequence results revealed that the dominant genera in the microbial agent were *Mesorhizobium* (54.2%) and *norank_f__norank_o__Chloroplast* (25.1%), both typical organic matter-degrading bacteria [48,49]. Experiments were conducted using an A^2/O reactor, with nitrogen removal efficiency shown in Figure 8. The denitrification efficiency in the anoxic tank consistently remained at relatively low levels. During operation, the removal efficiency of NO_3^--N from the recirculated nitrified liquid in the anoxic tank ranged from 5% to 30%. No external carbon source was added throughout reactor operation, relying solely on influent COD to provide carbon sources. The hydraulic retention time in the anoxic tank section reached 10.6 h, satisfying the theoretical time requirements for biological denitrification. Therefore, the poor denitrification performance in the anoxic tank was attributed to insufficient influent carbon sources.

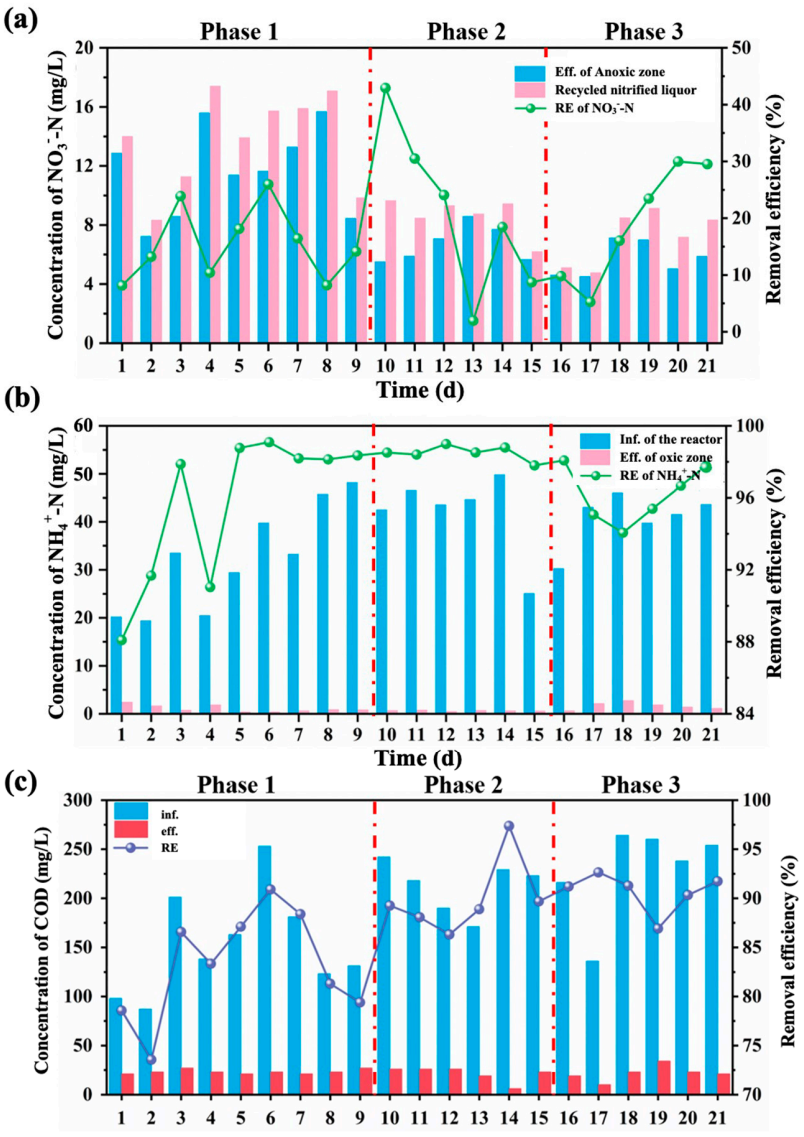

Figure 8. Effect of microbial agents on NO_3^--N removal performance in the anoxic tank (**a**), NH_4^+-N in the oxic tank (**b**), and COD removal performance (**c**).

After adding the EPS-optimizing microbial agent, the nitrogen removal efficiency gradually improved after a short period, indicating that the addition of EPS-optimizing microbial agents does not significantly impact the nitrogen removal performance. During the initial reactor operation phase, NH_4^+-N removal efficiency in the oxic tank was highly unstable. After stable operation, NH_4^+-N removal efficiency maintained approximately 98 ± 1.2%, indicating good nitrification performance in the oxic tank. After adding the EPS-optimizing microbial agents, NH_4^+-N removal efficiency in the oxic tank exhibited notable short-term fluctuations. Effluent NH_4^+-N exceeded 2 mg/L, and the removal efficiency temporarily decreased to 93 ± 2.1%. However, the removal efficiency recovered to above 96% within 4 days.

COD removal efficiency is shown in Figure 8c. On day 18, the reactor influent COD concentration reached its maximum at 264 mg/L, while the minimum of 87 mg/L occurred the following day, which was related to heavy rainfall during the initial reactor operation period. The lowest COD removal efficiency was less than 75% during the initial operation phase, and stabilized at approximately 90% after 10 days operation. Following the addition of EPS-optimizing microbial agents, COD removal efficiency remained at 90%, indicating that the addition of EPS-optimizing microbial agents does not affect microbial adsorption, degradation, and utilization of COD.

3.4.2. Variation of EPS Components

The PN and PS in EPS from different tanks were monitored before and after the addition of EPS-optimizing microbial agents (Figure 9). The PN in DOM of the anaerobic tank showed minimal changes, while the PN in LB-EPS and TB-EPS exhibited significant variations. During the pre-addition operation period, PN in LB-EPS and TB-EPS increased from 23.7 mg/gVSS and 59.4 mg/gVSS to 39.3 mg/gVSS and 78.9 mg/gVSS, respectively, representing increases of 65.8% and 32.8%. Following the addition of EPS-optimizing microbial agents, PN in LB-EPS and TB-EPS decreased to 11.7 mg/gVSS and 58.1 mg/gVSS, respectively, with reductions of 70.2% and 26.4%. The changes in PS in LB-EPS and TB-EPS were also notable. During the pre-addition operation period, PS contents increased from 1.74 mg/gVSS and 9.36 mg/gVSS to 3.01 mg/gVSS and 13.38 mg/gVSS, respectively, representing increases of 72.9% and 42.95%. After microbial agent addition, PS in LB-EPS and TB-EPS significantly decreased to 1.37 mg/gVSS and 7.11 mg/gVSS, with reductions of 54.5% and 46.9%, respectively.

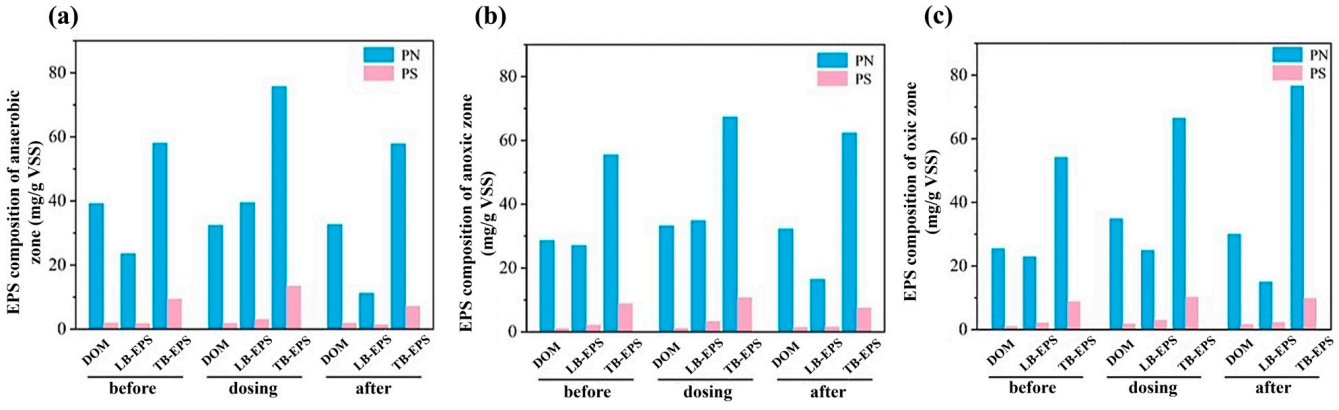

Figure 9. Changes in EPS content in anaerobic zone (**a**), anoxic zone (**b**), and oxic zone (**c**) before and after dosing microbial agents.

During operation, PN in LB-EPS and TB-EPS in the anoxic tank increased from 27.05 mg/gVSS and 55.45 mg/gVSS to 34.87 mg/gVSS and 67.35 mg/gVSS, respectively, representing increases of 28.9% and 21.5%. PN contents decreased to 16.46 mg/gVSS and 62.33 mg/gVSS, respectively, followed by an addition of microbial agent. After microbial agent addition, PS in LB-EPS and TB-EPS decreased to 1.53 mg/gVSS and 7.48 mg/gVSS, with reductions of 52.5% and 30.4%, respectively. Similarly, the overall changes in PN and PS contents in DOM of the oxic tank were minimal, while PN and PS in LB-EPS and TB-EPS showed significant changes before and after microbial agent addition. PN and PS in LB-EPS and TB-EPS decreased to 14.95 mg/gVSS and 2.28 mg/gVSS after microbial agent addition, with reductions of 39.9% and 23.0%, respectively. In conclusion, the addition of EPS-optimizing microbial agents can significantly reduce PN and PS in LB-EPS of all tanks, while having minimal effect on DOM contents in all tanks.

Figure 10 presents the three-dimensional fluorescence spectra of sludge EPS in the anoxic tank before and after the addition of EPS-optimizing microbial agents. It can be used to investigate protein-like substances, fulvic acids, and humic substances, and evaluate the biodegradability and utilization difficulty of various EPS components by microorganisms [50,51]. The regional fluorescence intensity proportions of extracellular polymeric substances in various regions of the anoxic tank were similar during the reactor stabilization period and on the day of microbial agent addition. Following microbial agent addition, the regional fluorescence intensities of various EPS regions exhibited considerable changes. Compared to pre-addition conditions, the fluorescence intensities of regions I, II, and III in DOM (protein-like substances and fulvic acid-like substances) significantly decreased after microbial agent addition. Regions IV and V (soluble microbial metabolic products and humic-like substances) showed notable increases. The fluorescence intensities of regions I and II (protein-like substances) in LB-EPS and TB-EPS decreased, while regions III and V (fulvic acids and humic-like substances) increased. This demonstrates that the addition of this microbial agent significantly affects the fluorescent substances in EPS. Except for the increases in regions III and V (fulvic acids and humic-like substances) of TB-EPS in the anoxic tank before and after microbial agent addition, all other proportions of protein-like substances decreased. Tyrosine, tryptophan, and soluble microbial metabolic products were utilized by microorganisms after microbial agent addition, with protein-like substances showing relatively high microbial utilization rates. Therefore, it can be inferred that adding this type of microbial agent during winter can reduce the accumulation of protein components in sludge EPS, thereby improving sludge settling performance.

The economic feasibility of EPS-optimizing microbial agents represents a critical factor for practical implementation. Based on our laboratory-scale results using a dosage of 2000 g/m^3, the estimated treatment cost would be approximately \$20/m^3 of treated wastewater. This cost must be weighed against the operational benefits, including reduced sludge handling costs due to improved settling performance, decreased chemical coagulant requirements, and potential energy savings from improved process stability. The microbial agents can be produced through standard fermentation processes, making scale-up feasible for most WWTPs. Further economic analysis and pilot-scale studies are recommended to optimize dosage strategies and reduce implementation costs.

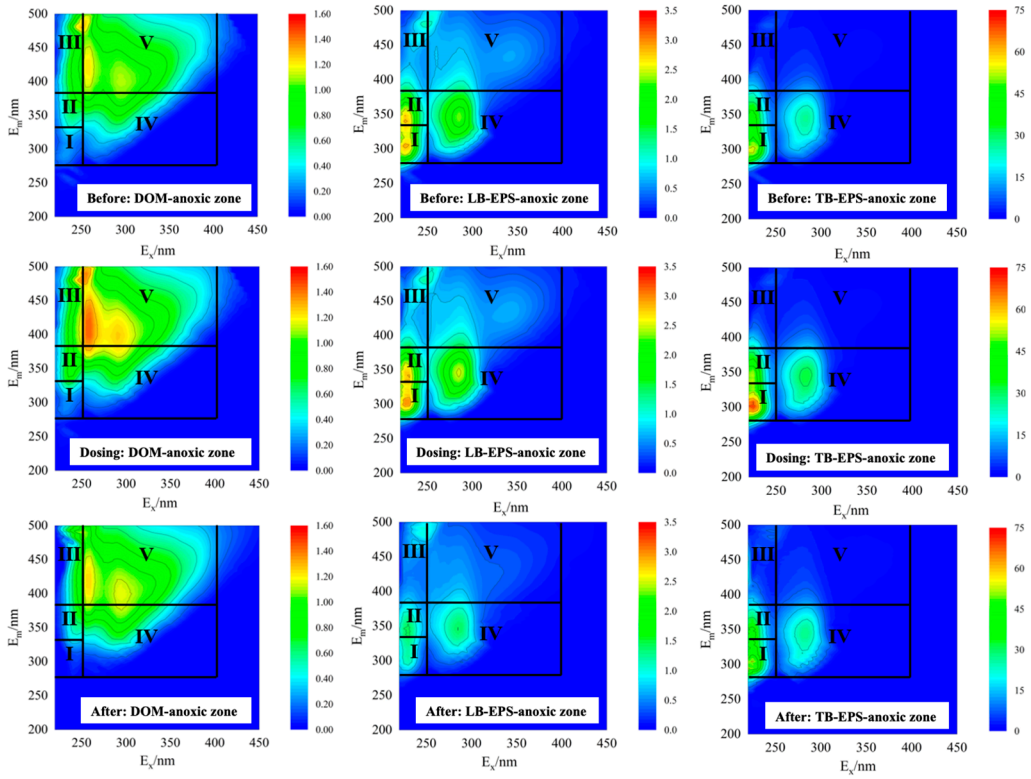

Figure 10. Fluorescence intensity (FI) changes of EPS in anoxic tank of reactor before and after dosing microbial agents.

4. Conclusions

This study elucidated the temperature–EPS interaction mechanisms affecting nitrogen removal performance in full-scale wastewater treatment systems. Water temperature variations significantly influenced nitrification and denitrification processes, with TB-EPS content decreasing substantially when temperatures dropped below 15 °C while DOM and LB-EPS increased, representing the primary cause of deteriorated sludge settling performance. The modified Bardenpho process demonstrated resilience to temperature fluctuations through enhanced substrate utilization efficiency. EPS-optimizing microbial agents effectively reduced PN component accumulation in sludge EPS without affecting COD removal efficiency, thereby improving sludge settling performance during cold wave impacts. These findings provide a fundamental understanding of seasonal performance variations and practical solutions for maintaining stable year-round operation of biological wastewater treatment systems under challenging temperature conditions.

Supplementary Materials: The following supporting information can be downloaded at: https://www.mdpi.com/article/10.3390/fermentation11090532/s1. Table S1: Illumina sequence sampling date of sludge; Figure S1: Proportion of fluorescence intensity (FI) in each region.

Author Contributions: Conceptualization, F.X.; Data curation, F.G.; Formal analysis, F.X. and L.J.; Funding acquisition, B.Z.; Investigation, F.X. and B.Z.; Methodology, F.X. and B.Z.; Project administration, F.X.; Resources, M.E.D.; Software, F.X.; Supervision, B.Z.; Validation, F.X., C.T. and L.J.; Visualization, F.X., L.J. and F.G.; Writing—original draft, F.X.; Writing—review & editing, X.M., L.J. and Z.Y. All authors have read and agreed to the published version of the manuscript.

Funding: This research was funded by the National Natural Science Foundation of China (No. 42177057), Shanxi Provincial Foundation Research Program (No. 202203021212299), Shanxi Provincial Key Research and Development Project (No. 202202140601019; 202302090301012).

Institutional Review Board Statement: Not applicable.

Informed Consent Statement: Not applicable.

Data Availability Statement: Data is contained within the article.

Acknowledgments: The authors thank other laboratory members for algal culture and technical assistance.

Conflicts of Interest: Authors Feng Gao and Zhihong Yang were employed by the company Shanxi Zhengyang Sewage Purification Co., Ltd. The remaining authors declare that the research was conducted in the absence of any commercial or financial relationships that could be construed as a potential conflict of interest.

References

1. Chen, G.; van Loosdrecht, M.C.M.; Ekama, G.A.; Brdjanovic, D. *Biological Wastewater Treatment: Principles, Modelling and Design*; IWA Publishing: London, UK, 2023. [CrossRef]
2. Li, W.; Sangeetha, T.; Han, X.; Yan, W.-M.; Yang, L.; Zhao, J.; Cai, W.; Yao, H. Tracking the diversity and interaction of methanogens in the energy recovery process of a full-scale wastewater treatment plant. *Environ. Res.* **2022**, *211*, 113010. [CrossRef]
3. Zhang, X.; Zhao, B.; Li, R.; Cui, Y.; Xie, F.; Zhou, A.; Li, J.; Yue, X. Study on the feasibility of carbon source recovery by upflow anaerobic sludge blanket in simulated municipal wastewater. *Sci. Total Environ.* **2023**, *878*, 163157. [CrossRef]
4. Liu, Z.; Zhang, X.; Zhang, S.; Qi, H.; Hou, Y.; Gao, M.; Wang, J.; Zhang, A.; Chen, Y.; Liu, Y. A comparison between exogenous carriers enhanced aerobic granulation under low organic loading in the aspect of sludge characteristics, extracellular polymeric substances and microbial communities. *Bioresour. Technol.* **2022**, *346*, 126567. [CrossRef] [PubMed]
5. Revollar, S.; Meneses, M.; Vilanova, R.; Francisco, M.; Vega, P. Adapting WWTP performance to seasonality and climate change: Temperature-driven strategies for enhanced nitrogen removal. *Process Saf. Environ. Prot.* **2025**, *195*, 106792. [CrossRef]
6. Wang, P.; Yu, Z.; Qi, R.; Zhang, H. Detailed comparison of bacterial communities during seasonal sludge bulking in a municipal wastewater treatment plant. *Water Res.* **2016**, *105*, 157–166. [CrossRef]
7. Yuan, F.; Liu, M.; Sun, H.; Feng, Z.; Liu, X.; Dong, X.; Zhao, S.; Ding, J.; Chen, Y. Low-temperature sludge bulking in wastewater treatment plants: Causal analysis and mechanistic investigation. *J. Water Process Eng.* **2025**, *76*, 108233. [CrossRef]
8. Cong, S.; Yu, G.; Xia, S.; Yu, H.; Sun, Y.; Gao, Y.; Liu, Y.; Zou, D. Pilot–scale vertical continuous–flow reactors applied to treat rural domestic wastewater at low temperature via aerobic granular sludge. *J. Water Process Eng.* **2024**, *60*, 105220. [CrossRef]
9. Peng, S.; Hu, A.; Ai, J.; Zhang, W.; Wang, D. Changes in molecular structure of extracellular polymeric substances (EPS) with temperature in relation to sludge macro-physical properties. *Water Res.* **2021**, *201*, 117316. [CrossRef]
10. Sam, S.B.; Ward, B.J.; Niederdorfer, R.; Morgenroth, E.; Strande, L. Elucidating the role of extracellular polymeric substances (EPS) in dewaterability of fecal sludge from onsite sanitation systems, and changes during anaerobic storage. *Water Res.* **2022**, *222*, 118915. [CrossRef]
11. Jin, B.; Wilén, B.-M.; Lant, P. Impacts of morphological, physical and chemical properties of sludge flocs on dewaterability of activated sludge. *Chem. Eng. J.* **2004**, *98*, 115–126. [CrossRef]
12. Mikkelsen, L.H.; Keiding, K. Physico-chemical characteristics of full scale sewage sludges with implications to dewatering. *Water Res.* **2002**, *36*, 2451–2462. [CrossRef]
13. Wingender, J.; Neu, T.R.; Flemming, H.-C. What are Bacterial Extracellular Polymeric Substances? In *Microbial Extracellular Polymeric Substances: Characterization, Structure and Function*; Wingender, J., Neu, T.R., Flemming, H.-C., Eds.; Springer: Berlin/Heidelberg, Germany, 1999; pp. 1–19.
14. Liang, S.; Liu, C.; Song, L. Soluble microbial products in membrane bioreactor operation: Behaviors, characteristics, and fouling potential. *Water Res.* **2007**, *41*, 95–101. [CrossRef] [PubMed]
15. Aquino, S.F.; Stuckey, D.C. Soluble microbial products formation in anaerobic chemostats in the presence of toxic compounds. *Water Res.* **2004**, *38*, 255–266. [CrossRef]
16. Ni, B.-J.; Rittmann, B.E.; Yu, H.-Q. Soluble microbial products and their implications in mixed culture biotechnology. *Trends Biotechnol.* **2011**, *29*, 454–463. [CrossRef]
17. Raszka, A.; Chorvatova, M.; Wanner, J. The role and significance of extracellular polymers in activated sludge. Part I: Literature review. *Acta Hydroch. Hydrob.* **2006**, *34*, 411–424. [CrossRef]
18. Ben Hamed, H.; Mainardis, M.; Moretti, A.; Toye, D.; Léonard, A. Extracellular polymeric substances (EPS) in sewage sludge management: A call for methodological standardization. *J. Environ. Manag.* **2025**, *376*, 124407. [CrossRef] [PubMed]
19. Chen, Y.; Liu, Y.; Lv, J.; Wu, D.; Jiang, L.; Lv, W. Short-time aerobic digestion treatment of waste activated sludge to enhance EPS production and sludge dewatering performance by changing microbial communities: The impact of temperature. *Water Cycle* **2024**, *5*, 146–155. [CrossRef]

20. Pérez-Sancho, M.; Vela, A.I.; Wiklund, T.; Kostrzewa, M.; Domínguez, L.; Fernández-Garayzábal, J.F. Differentiation of Flavobacterium psychrophilum from Flavobacterium psychrophilum-like species by MALDI-TOF mass spectrometry. *Res. Vet. Sci.* **2017**, *115*, 345–352. [CrossRef]
21. Sun, H.-J.; Zhao, X.; Ding, J.; Wang, Y.-Q.; Wang, W.-S.; Feng, Z.-H.; Zhao, S.; Wang, L.; Ren, N.-Q.; Yang, S.-S. Unveiling dynamics of microbial communities, species interactions, and ecological assembly during low-temperature-induced sludge bulking in full-scale wastewater treatment systems. *Bioresour. Technol.* **2025**, *435*, 132950. [CrossRef]
22. Ranieri, E.; D'Onghia, G.; Lopopolo, L.; Gikas, P.; Ranieri, F.; Gika, E.; Spagnolo, V.; Herrera, J.A.; Ranieri, A.C. Influence of climate change on wastewater treatment plants performances and energy costs in Apulia, south Italy. *Chemosphere* **2024**, *350*, 141087. [CrossRef]
23. Zhao, B.; Xie, F.; Zhou, A.; Liu, Z.; Ji, L.; Zhang, G.; Yue, X. Analysis of energy recovery and microbial community in an amalgamated CSTR-UASBs reactor for a three-stage anaerobic fermentation process of cornstalks. *Water Sci. Technol.* **2022**, *86*, 1848–1857. [CrossRef]
24. Walter, W. APHA Standard Methods for the Examination of Water and Wastewater. *Am. J. Public Health Nations Health* **1961**, *51*, 940. [CrossRef]
25. Bian, X.; Wu, Y.; Li, J.; Yin, M.; Li, D.; Pei, H.; Chang, S.; Guo, W. Effect of dissolved oxygen on high C/N wastewater treatment in moving bed biofilm reactors based on heterotrophic nitrification and aerobic denitrification: Nitrogen removal performance and potential mechanisms. *Bioresour. Technol.* **2022**, *365*, 128147. [CrossRef]
26. SEPA. State Environmental Protection Administration, the People's Republic of China. Discharge Standard of Pollutants for Municipal Wastewater Treatment Plant (GB 18918–2002). 2002. Available online: https://www.mee.gov.cn/ywgz/fgbz/bz/bzwb/shjbh/swrwpfbz/200307/t20030701_66529.shtml (accessed on 26 July 2025).
27. Tkach, O.; Sangeetha, T.; Maria, S.; Wang, A. Performance of low temperature Microbial Fuel Cells (MFCs) catalyzed by mixed bacterial consortia. *J. Environ. Sci.* **2017**, *52*, 284–292. [CrossRef]
28. Xie, Y.; Zhang, Q.; Wu, Q.; Zhang, J.; Dzakpasu, M.; Wang, X.C. Advancing nitrogen removal in low-temperature sewage treatment: Role of the adaptive activated sludge process. *Chem. Eng. J.* **2025**, *504*, 158887. [CrossRef]
29. Li, B.; Godfrey, B.J.; RedCorn, R.; Candry, P.; Abrahamson, B.; Wang, Z.; Goel, R.; Winkler, M.-K.H. Mainstream nitrogen removal from low temperature and low ammonium strength municipal wastewater using hydrogel-encapsulated comammox and anammox. *Water Res.* **2023**, *242*, 120303. [CrossRef]
30. Xiong, X.; Yang, N.; Liu, M.; Jiang, X.; Luo, D.; Lei, Y. Resilience of electroactive pollutant removal and power generation to long-term temperature shifts in domestic wastewater treatment during the autumn-winter-spring period. *J. Environ. Chem. Eng.* **2025**, *13*, 117386. [CrossRef]
31. Wang, L.; Yuan, L.; Li, Z.-H.; Zhang, X.; Leung, K.M.Y.; Sheng, G.-P. Extracellular polymeric substances (EPS) associated extracellular antibiotic resistance genes in activated sludge along the AAO process: Distribution and microbial secretors. *Sci. Total Environ.* **2022**, *816*, 151575. [CrossRef] [PubMed]
32. More, T.T.; Yadav, J.S.S.; Yan, S.; Tyagi, R.D.; Surampalli, R.Y. Extracellular polymeric substances of bacteria and their potential environmental applications. *J. Environ. Manag.* **2014**, *144*, 1–25. [CrossRef] [PubMed]
33. Melo, A.; Costa, J.; Quintelas, C.; Amaral, A.L.; Ferreira, E.C.; Mesquita, D.P. Quantitative image analysis for assessing extracellular polymeric substances in activated sludge under atrazine exposure. *Sep. Purif. Technol.* **2024**, *349*, 127831. [CrossRef]
34. Ma, X.; Zhao, B.; Zhang, X.; Xie, F.; Cui, Y.; Li, H.; Yue, X. Effect of periodic temperature shock on nitrogen removal performance and microbial community structure in plug-flow microaerobic sludge blanket. *Chemosphere* **2020**, *241*, 124934. [CrossRef]
35. Cao, S.; Du, R.; Li, B.; Ren, N.; Peng, Y. High-throughput profiling of microbial community structures in an ANAMMOX-UASB reactor treating high-strength wastewater. *Appl. Microbiol. Biotechnol.* **2016**, *100*, 6457–6467. [CrossRef]
36. Kono, M.; Haruta, S. Coaggregation Occurs between a Piliated Unicellular Cyanobacterium, Thermosynechococcus, and a Filamentous Bacterium, *Chloroflexus aggregans*. *Microorganisms* **2024**, *12*, 1904. [CrossRef]
37. Zhao, Y.; Jiang, B.; Tang, X.; Liu, S. Metagenomic insights into functional traits variation and coupling effects on the anammox community during reactor start-up. *Sci. Total Environ.* **2019**, *687*, 50–60. [CrossRef]
38. Zhao, J.-Y.; Geng, S.; Xu, L.; Hu, B.; Sun, J.-Q.; Nie, Y.; Tang, Y.-Q.; Wu, X.-L. Complete genome sequence of Defluviimonas alba cai42T, a microbial exopolysaccharides producer. *J. Biotechnol.* **2016**, *239*, 9–12. [CrossRef] [PubMed]
39. Zhang, Y.; Qiao, Y.; Fu, Z. Shifts of bacterial community and predictive functional profiling of denitrifying phosphorus removal—Partial nitrification—Anammox three-stage nitrogen and phosphorus removal before and after coupling for treating simulated wastewater with low C/N. *Chem. Eng. J.* **2023**, *451*, 138601. [CrossRef]
40. Liu, H.; Zeng, W.; Meng, Q.; Fan, Z.; Peng, Y. Phosphorus removal performance, intracellular metabolites and clade-level community structure of Tetrasphaera-dominated polyphosphate accumulating organisms at different temperatures. *Sci. Total Environ.* **2022**, *842*, 156913. [CrossRef]
41. Liu, R.; Chen, Y.; Li, S.-Y.; Chen, Y.-P.; Guo, J.-S.; Liu, S.-Y.; Yan, P. Filamentous bacteria in activated sludge: Geographic distribution and impact of treatment processes. *J. Environ. Manag.* **2025**, *379*, 124859. [CrossRef]

42. Wang, K.; Zhou, C.; Zhou, H.; Jiang, M.; Chen, G.; Wang, C.; Zhang, Z.; Zhao, X.; Jiang, L.-M.; Zhou, Z. Comparison on biological nutrient removal and microbial community between full-scale anaerobic/anoxic/aerobic process and its upgrading processes. *Bioresour. Technol.* **2023**, *374*, 128757. [CrossRef]
43. Shi, W.; He, Z.; Lu, J.; Wang, L.; Guo, J.; Qiu, S.; Ge, S. Response of nitrifiers to gradually increasing pH conditions in a membrane nitrification bioreactor: Microbial dynamics and alkali-resistant mechanism. *Water Res.* **2025**, *268*, 122567. [CrossRef]
44. Liu, Q.; Liao, X.; Li, Y.; Zhang, M.; Li, J. Reduction of chromate and nitrate by type II aerobic methanotrophs under micro-aerobic conditions. *Chem. Eng. J.* **2025**, *505*, 159286. [CrossRef]
45. Liu, Z.; Cui, Z.; Guo, Z.; Li, D.; He, Z.; Liu, W.; Yue, X.; Zhou, A. Insights into the effect of nitrate photolysis on short-chain fatty acids production from waste activated sludge in anaerobic fermentation system: Performance and mechanisms. *Water Res.* **2024**, *258*, 121772. [CrossRef]
46. Sun, J.; Pan, F.; Zhu, H.; Wu, Q.; Pan, C.; Lu, F. Enhancing low-temperature anaerobic digestion of low-strength organic wastewater through bio-electrochemical technology. *Int. J. Hydrogen Energy* **2024**, *58*, 1062–1074. [CrossRef]
47. Xu, L.; Li, L.; Liu, J.; Wang, X.; Zhao, Y.; Zhao, J.; Gu, L.; He, Q.; Wang, X.; Zhang, J. Ferrihydrite optimizing Feammox inoculum to enhance ammonia removal from concentrate wastewater through continuous upflow anaerobic sludge blanket (UASB). *J. Environ. Chem. Eng.* **2024**, *12*, 114469. [CrossRef]
48. Gao, L.; Wang, S.; Xu, X.; Zheng, J.; Cai, T.; Jia, S. Metagenomic analysis reveals the distribution, function, and bacterial hosts of degradation genes in activated sludge from industrial wastewater treatment plants. *Environ. Pollut.* **2024**, *340*, 122802. [CrossRef]
49. Zhang, S.; Chen, J.; Sang, W.; Li, M.; Prodanovic, V.; Zhang, K. Metagenomic insights into the explanation of biofilter performance distinction induced by dissolved oxygen increment. *Process Saf. Environ. Prot.* **2021**, *153*, 329–338. [CrossRef]
50. Tian, W.; Li, L.; Liu, F.; Zhang, Z.; Yu, G.; Shen, Q.; Shen, B. Assessment of the maturity and biological parameters of compost produced from dairy manure and rice chaff by excitation–emission matrix fluorescence spectroscopy. *Bioresour. Technol.* **2012**, *110*, 330–337. [CrossRef]
51. Zhen, G.; Lu, X.; Wang, B.; Zhao, Y.; Chai, X.; Niu, D.; Zhao, A.; Li, Y.; Song, Y.; Cao, X. Synergetic pretreatment of waste activated sludge by Fe(II)–activated persulfate oxidation under mild temperature for enhanced dewaterability. *Bioresour. Technol.* **2012**, *124*, 29–36. [CrossRef]